

Genetic control of HDL levels and composition in an interspecific mouse cross (CAST/Ei × C57BL/6J)

Margarete Mehrabian,* Lawrence W. Castellani,* Ping-Zi Wen,* Jack Wong,* Tat Rithaporn,[†] Susan Y. Hama,* Gregory P. Hough,* David Johnson,* John J. Albers,^{††} Giuliano A. Mottino,* Joy S. Frank,* Mohamad Navab,* Alan M. Fogelman,* and Aldons J. Lusis^{1,*†,§,**}

Department of Medicine,* Department of Microbiology and Molecular Genetics,[†] Department of Human Genetics,[§] and Molecular Biology Institute,^{**} University of California, Los Angeles, CA 90095, and Northwest Lipid Laboratories,^{††} Department of Medicine, University of Washington, Seattle, WA 98115

Abstract Strain CAST/Ei (CAST) mice exhibit unusually low levels of high density lipoproteins (HDL) as compared with most other strains of mice, including C57BL/6J (B6). This appears to be due in part to a functional deficiency of lecithin:cholesterol acyltransferase (LCAT). LCAT mRNA expression in CAST mice is normal, but the mice exhibit several characteristics consistent with functional deficiency. First, the activity and mass of LCAT in plasma and in HDL of CAST mice were reduced significantly. Second, the HDL of CAST mice were relatively poor in phospholipids and cholesteryl esters, but rich in free cholesterol and apolipoprotein A-I (apoA-I). Third, the adrenals of CAST mice were depleted of cholesteryl esters, a phenotype similar to that observed in LCAT- and acyl-CoA:cholesterol acyltransferase-deficient mice. Fourth, in common with LCAT-deficient mice, CAST mice contained triglyceride-rich lipoproteins with “panhandle”-like protrusions. To examine the genetic bases of these differences, we studied HDL lipid levels in an intercross between strain CAST and the common laboratory strain B6 on a low fat, chow diet as well as a high fat, atherogenic diet. HDL levels exhibited complex inheritance, as 12 quantitative trait loci with significant or suggestive likelihood of observed data scores were identified. Several of the loci occurred over plausible candidate genes and these were investigated. **■** The results indicate that the functional LCAT deficiency is unlikely to be due to variations of the LCAT gene. Our results suggest that novel genes are likely to be important in the control of HDL metabolism, and they provide evidence of genetic factors influencing the interaction of LCAT with HDL.—Mehrabian, M., L. W. Castellani, P-Z. Wen, J. Wong, T. Rithaporn, S. Y. Hama, G. P. Hough, D. Johnson, J. J. Albers, G. A. Mottino, J. S. Frank, M. Navab, A. M. Fogelman, and A. J. Lusis. **Genetic control of HDL levels and composition in an interspecific mouse cross (CAST/Ei × C57BL/6J).** *J. Lipid Res.* 2000. 41: 1936–1946.

Supplementary key words quantitative trait locus mapping • lecithin:cholesterol acyltransferase • adrenal lipid depletion • scavenger receptor BI • phospholipid transfer protein • apolipoprotein A-I • cholesterol-7 α -hydroxylase • high fat diet

The inverse relationship between high density lipoprotein (HDL) levels and coronary artery disease (CAD) (1) has generated interest in the metabolism of HDL and the environmental and genetic factors contributing to variations in HDL levels. The major structural proteins of HDL are apolipoprotein A-I (apoA-I) and apoA-II, but HDL also contains numerous other proteins, including lecithin:cholesterol acyl-transferase (LCAT), serum paraoxonase (PON1), platelet-activating factor acetylhydrolase (PAF-AH), apoE, apoA-IV, cholesteryl ester transfer protein (CETP), and phospholipid transfer protein (PLTP). HDL are extremely heterogeneous, and various species of HDL differ in functions relevant to CAD, such as the ability to promote cholesterol efflux and to inhibit LDL oxidation (2). Biochemical and physiologic studies have revealed that HDL are derived from the transfer of surface components of triglyceride-rich lipoproteins into HDL (3, 4) and from the association of cellular plasma membranes with apoA-I (3, 5). Studies of human mutations and transgenic/knock-out mice have clarified the functions of various HDL proteins in vivo. Human metabolic studies have also indicated that common variations in HDL cholesterol levels are strongly related to the fractional catabolic rate of apoA-I (6). However, the genetic factors contributing to common variation in HDL levels and functional differences among human populations are poorly understood. One significant genetic determinant of HDL levels is a polymorphism of the promoter region of hepatic lipase, which contributes to HDL levels in males (7). The identification

Abbreviations: apoA-I, apolipoprotein A-I; ATH, atherogenic; B6, C57BL/6J; CAST, CAST/Ei; CAD, coronary artery disease; CETP, cholesteryl ester transfer protein; GAPDH, glyceraldehyde-3-phosphate dehydrogenase; HDL, high density lipoprotein; LCAT, lecithin:cholesterol acyltransferase; LOD, likelihood of the observed data; PAF-AH, platelet-activating factor acetylhydrolase; PCR, polymerase chain reaction; PLTP, phospholipid transfer protein; PON1, serum paraoxonase; QTLs, quantitative trait loci; SR-BI, scavenger receptor class B type I; UC/TC, unesterified cholesterol/total cholesterol.

¹ To whom correspondence should be addressed.

of the ATPase-binding cassette transporter responsible for Tangier disease has revealed a novel pathway for HDL metabolism, and some evidence suggests that variations of the transporter could contribute to common HDL deficiencies (8–10).

We now report studies of the genetic control of HDL levels in a mouse animal model. The mouse has become increasingly useful for the study of complex traits. As compared with human studies, the use of animal models reduces the effects of environmental variables and greatly simplifies linkage analysis (11). Common laboratory inbred strains of mice exhibit variations in HDL levels, functions, and structures (12), and we have previously reported biochemical and genetic studies of some of these variations (13–21). In the present study, we have examined the genetic control of HDL levels in an intercross between the laboratory strain C57BL/6J (B6) and the distantly related (~1 million years) strain CAST/Ei (CAST), which is derived from a separate subspecies of mouse. These studies were performed with two different diets, one a low fat, chow diet and the other a high fat, atherogenic diet, to examine genetic-dietary interactions. The results have revealed a complex pattern of inheritance, with more than a dozen loci contributing to HDL levels and compositions on the two diets. Candidate genes at some of the loci were examined for possible involvement. The results suggest that a significant proportion of the genetic component in HDL metabolism is unlikely to be explained by the usual candidates for plasma lipid metabolism. They also reveal that CAST mice have low HDL levels due, in part, to reduced LCAT activity, and that this, in turn, results in a form of adrenal lipid depletion. Interestingly, the low LCAT activity is not due to reduced LCAT expression, but, apparently, to a genetic factor influencing the interaction of LCAT with HDL.

MATERIALS AND METHODS

Mice

All mice were purchased from the Jackson Laboratory (Bar Harbor, ME) and were housed under conditions meeting Association for Assessment and Accreditation of Laboratory Animal Care. CAST males were mated with B6 females and the resulting F₁ progeny were intercrossed to produce the F₂ progeny. The F₂ mice were weaned at about 21 days of age onto rodent chow containing 6% of calories from fat (Purina 5001) and at about 4 months of age, they were switched to a high fat, high cholesterol diet for 5 weeks. This diet was 75% chow supplemented with 7.5% cocoa butter (resulting in 15% of calories from fat) and also 2.5% dextrose, 1.625% each of sucrose and dextrin, 1.25% cholesterol, and 0.05% sodium cholate (Diet No. 90221; Harlan Teklad, Madison, WI). The mice were given ad libitum access to food and were maintained on a 12-h light-dark cycle throughout.

Quantitation of plasma lipids and body fat

Briefly, mice were fasted overnight before collection of blood and were killed ~3 h into the diurnal phase of the light cycle. The kidneys, liver, and adrenals were collected for DNA isolation and other analyses. Plasma lipoproteins were separated, and lipids were quantitated using enzymatic procedures as previously de-

scribed (15). LCAT activity and PLTP activity in plasma were determined as previously described (22, 23).

Lipoprotein isolation

Mouse lipoproteins were isolated either by density ultracentrifugation or by fast performance liquid chromatography (FPLC) (24). For FPLC, 450 μ l of pooled heparinized plasma was injected onto two Pharmacia (Uppsala, Sweden) Superose 6 columns connected in series, and lipoproteins eluted with 154 mM NaCl and 3 mM sodium azide in endotoxin-free water, pH 8.2. Fractions of 1.0 ml each were collected. The lipoprotein elution profile was determined by measuring cholesterol, and appropriate fractions were pooled. Cholesterol was determined by an enzymatic assay as described (15). The pooled lipoproteins were filtered through molecular weight cutoff (CUFC4) filters to remove the sodium azide present in the FPLC effluent (Millipore, Boston, MA).

Isolation of liver membrane for SR-BI quantitation

Mouse liver membranes were prepared by homogenizing 1 g of liver in 10 ml of 150 mM NaCl, 1 mM CaCl₂, 10 mM Tris-HCl (pH 7.5), 0.5 μ M leupeptin, 1 mM phenylmethylsulfonyl fluoride, pH 7.5 (buffer A). A low speed supernatant was first prepared by centrifuging the homogenate at 500 *g* for 5 min and then at 8,000 *g* for 15 min. The supernatant was then spun at 100,000 *g* (24,000 rpm in an SW40Ti rotor) for 1 h and the supernatant was discarded. The pellet was suspended in 1 ml of buffer A by flushing 10 times through a 1-ml syringe with a 22-gauge needle. The dispersed pellet was transferred to a new ultracentrifuge tube, 4 ml of buffer A was added, and the mixture was spun at 100,000 *g* for 60 min. The supernatant was discarded and the pellet was resuspended in 0.5 ml of 50 mM NaCl, 1 mM CaCl₂, and 20 mM Tris-HCl, pH 7.5. Protein concentrations were determined by the Bio-Rad (Hercules, CA) dye-binding protein assay.

Immunoblotting analyses

Protein electrophoresis was carried out using Novex (San Diego, CA) NuPAGE 4–12% precast polyacrylamide gradient gels either under reducing or nonreducing conditions as described by Novex. Proteins were transferred onto nitrocellulose membranes and visualized by enhanced chemiluminescence (ECL) detection (Amersham, Little Chalfont, Buckinghamshire, UK). Quantification of the specific luminescent protein bands was performed with Image-Quant software (Molecular Dynamics, Sunnyvale, CA). For scavenger receptor class B type I (SR-BI) immunoblotting, 10 μ g of solubilized liver membranes was subjected to electrophoresis and transferred to filters, and incubated overnight with a 1:2,000 dilution of mouse SR-BI antibody (provided by M. C. deBeer, University of Kentucky, Lexington, KY). For LCAT immunoblotting, a 1:500 dilution of human LCAT antibody (Data Medical Associates, Arlington, TX) was used to detect LCAT protein in either mouse plasma (2 μ l), isolated HDL prepared by density ultracentrifugation (0.5 μ g total protein), or FPLC fractions (10 μ l). Antibodies against mouse apoA-I or apoE were purchased from Biodesign International (Kennebunk, ME) and used at dilutions of 1:5,000 and 1:1,000, respectively. For apoD immunoblotting, a 1:500 dilution of human apoD antibody (Cortex Biochem, San Leandro, CA) was used to detect apoD in 1–3 μ l of mouse plasma.

mRNA isolation and Northern blotting

Total RNA was isolated from liver according to the Trizol reagent protocol (Gibco, Life Technologies, Grand Island, NY). Northern blot analysis was used to quantitate the mRNA levels of LCAT. For each sample, 15 μ g of RNA was electrophoresed through formaldehyde-1% agarose gels and transferred to 20 \times

TABLE 1. Comparison of HDL levels and related parameters in CAST and B6 mice on two diets

| Trait | Chow Diet (mean ± SE) | | Atherogenic Diet (mean ± SE) | |
|--------------------------------|-----------------------|--------------|------------------------------|-------------|
| | B6 | CAST | B6 | CAST |
| HDL cholesterol (mg/dl) | 54 ± 7 | 41 ± 2* | 30 ± 2 | 18 ± 2* |
| Paraoxonase (activity) | 82 ± 16 | 60 ± 9 | 43 ± 3 | 19 ± 2* |
| LCAT mRNA (relative units) | 5.5 ± 0.7 | 4.4 ± 0.8 | 4.1 ± 0.3 | 3.7 ± 0.5 |
| LCAT activity (units) | 48.6 ± 0.3 | 31.3 ± 0.2* | 20.2 ± 0.2 | 1.0 ± 0.1* |
| PAF-AH activity (units) | 6.3 ± 0.3 | 6.2 ± 0.7 | 6.9 ± 0.2 | 6.4 ± 0.3 |
| PLTP activity (units) | 10.4 ± 1.3 | 2.9 ± 0.3* | 11.6 ± 2.6 | 4.8 ± 0.4* |
| Plasma cholesterol (mg/dl) | 68 ± 6 | 63 ± 2 | 125 ± 15 | 764 ± 18* |
| Plasma triglyceride (mg/dl) | 123 ± 10 | 49 ± 9* | 65 ± 9 | 244 ± 32* |
| Plasma apoA1 (mg/dl) | 119 ± 7 | 98 ± 8 | 98 ± 18 | 99 ± 13 |
| Plasma UC/TC | 0.14 ± 0.01 | 0.37 ± 0.02* | 0.17 ± 0.01 | 0.28 ± 0.0* |
| HDL UC/TC | 0.22 ± 0.01 | 0.25 ± 0.01 | 0.20 ± 0.01 | 0.30 ± 0.01 |
| CYP7A1 mRNA (relative units) | 1.3 ± 0.3 | 2.0 ± 0.6 | 0.4 ± 0.1 | 1.2 ± 0.1 |
| SR-BI mRNA (relative units) | 1.5 ± 0.2 | 0.9 ± 0.1* | 3.3 ± 0.0 | 1.9 ± 0.0* |
| SR-BI protein (relative units) | 1.8 ± 0.1 | 1.7 ± 0.2 | 1.2 ± 0.0 | 1.0 ± 0.0 |

Abbreviations: HDL, high density lipoprotein; UC, unesterified cholesterol; TC, total cholesterol; CYP7A1, cytochrome P450 7A (cholesterol 7 α -hydroxylase).

Female mice 4–6 months of age were studied on a chow diet or after feeding an atherogenic diet for 5 weeks. Values represent the means of three to seven independent measurements. Levels significantly different ($P < 0.05$) between CAST and B6 mice are indicated with an asterisk (*).

SSC-equilibrated Hybond ECL nitrocellulose membranes. Membranes were hybridized after UV cross-linking and washed at a high stringency (65°C, 0.1 \times SSC). Northern blots were probed with a ³²P-labeled mouse LCAT polymerase chain reaction (PCR) product. The forward primer was 5'-GGGTGCTGTGCTGT TGG-3'; and the reverse primer was 5'-TGCCAAAGCCAGGGA CAC-3'. The blots were also hybridized with glyceraldehyde-3-phosphate dehydrogenase (GAPDH) cDNA to normalize the quantities of RNA loaded onto the gel lanes.

Linkage and data analyses

A complete linkage map for all chromosomes except the Y chromosome was constructed with microsatellite markers and restriction fragment length variants as previously described (21). PCR primers for microsatellite typing were purchased from Research Genetics (Huntsville, AL). Linkage maps were constructed with the Map Manager version 2.6.5 (25) program. Statistical comparison of quantitative traits between groups, as shown in the tables, was performed by analysis of variance and regression (Statview 4.5; Abacus Concepts, Berkeley, CA). Likelihood of the observed data (LOD) scores for quantitative traits were calculated with the MAPMAKER/QTL program (26). The data were adjusted for the effects of age and sex by regression.

Electron microscopy

Negatively stained lipid preparations were made by placing a drop of lipid solution onto a copper grid (300 mesh). Uranyl acetate stain was gently added to the drop and incubated for 3–5 min. After this time excess fluid was wicked off the grid, which was allowed to dry and then viewed in a JEOL (Tokyo, Japan) 100CX electron microscope. Two samples from CAST and B6 on both a chow and high fat diet were prepared. Fifty different grid squares for each sample were examined.

Sequence analyses of SR-BI, LCAT, and apoA-I from B6 and CAST mice

cDNA was prepared from total liver RNA of CAST and B6 mice, using random hexamers. Overlapping PCR primers were designed using OLIGO, a primer analysis program by Molecular Biology Insights (Cascade, CO; <http://www.olygo.net>). Fragments were then PCR amplified in 1.5 mM MgCl₂ buffer, using a “touchdown” protocol with temperatures ranging from 68 to 50°C. The products were purified and sequenced with an Ap-

plied Biosystems (Foster City, CA) automated sequencer. The results were analyzed by several sequencing programs: BLAST and Entrez at <http://www.ncbi.nlm.nih.gov>; CAP3, a sequencing assembly programming algorithm at <http://gcg.tigem.it/ASSEMBLY/>

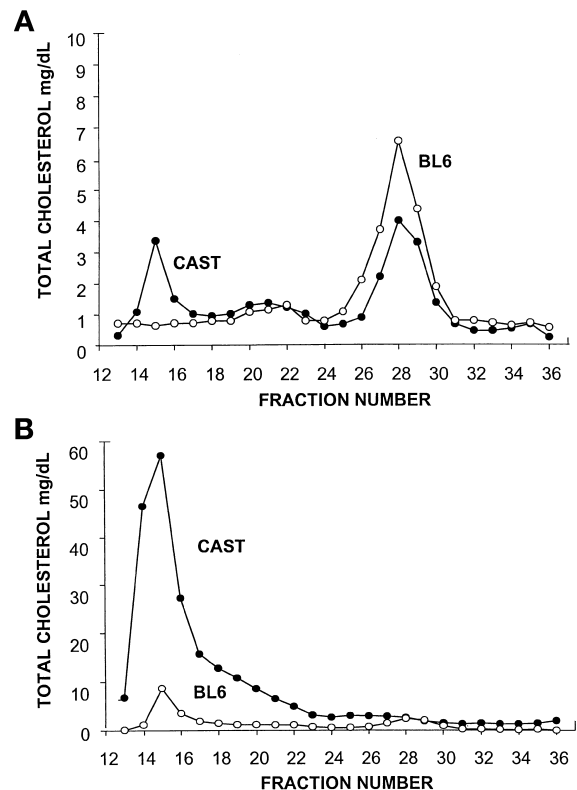


Fig. 1. Comparison of fast performance liquid chromatography (FPLC) profiles of plasma lipoproteins of CAST and B6 mice on chow (A) and atherogenic (B) diets. Plasma was collected from mice after an overnight fast. Plasma samples from five female mice of each strain were pooled and subjected to FPLC fractionation. Individual fractions were then assayed for cholesterol levels. Very low, intermediate, and low density lipoprotein eluted in fractions 18–24 while high density lipoprotein eluted in fractions 25–31.

assemble.html; and Genedoc at <http://www.cris.com/~ketchup/genedoc.shtml>. The translations into six reading frames were performed with the Baylor College of Medicine (Houston, TX) sequence analysis programs at their Website <http://dot.imgen.bcm.tmc.edu:9331/seq-util/seq-util.html>.

RESULTS

CAST mice have an unusual HDL profile and composition

Among various strains of mice surveyed (12), CAST are exceptional in their low levels of HDL cholesterol on a chow diet as well as a high fat, atherogenic diet containing cholic acid (Table 1). Most strains of mice, such as BALB/c and C3H, maintain relatively high levels of HDL cholesterol (70–90 mg/dl) on an atherogenic diet whereas CAST mice and B6 mice exhibit about a 2-fold decrease (Table 1). We have previously proposed that the decrease in HDL cholesterol in strain C57BL/6J mice in response to the atherogenic diet is related to decreased expression of cholesterol 7 α -hydroxylase (CYP7A1) (20). The results with CAST mice are consistent with this, because CAST mice also exhibited a decrease in CYP7A1 mRNA levels (Table 1). The FPLC lipoprotein profile of CAST mice is shown in Fig. 1. In addition to these differences in HDL levels, CAST mice were unusually responsive to an atherogenic diet in terms of the levels of low density lipoprotein/very high density lipoprotein (LDL/VLDL) cholesterol (Fig. 1). In genetic studies, described below, HDL levels did not cosegregate with LDL/VLDL levels, indicating that the low HDL and high LDL/VLDL in CAST mice result, at least in part, from independent genetic factors.

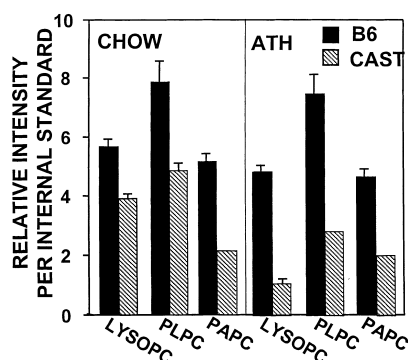


Fig. 2. High density lipoprotein (HDL) from CAST mice exhibit reduced levels of total phospholipids. HDL were ultracentrifugally isolated from CAST and B6 mice, maintained on either chow or atherogenic diets, and analyzed by positive ion mass spectrometry for the presence of certain phospholipids. A total of 25 μ g of HDL protein was injected in each experiment. The native phospholipid species analyzed in the HDL were lysophosphatidylcholine (lysoPC; $m/z = 496.2$), palmitoyl linolyl phosphatidylcholine (PLPC; $m/z = 758.3$), and palmitoyl arachidonoyl phosphatidylcholine (PAPC; $m/z = 782.3$). Chow diet: lysoPC, $P \leq 0.05$; PLPC, $P \leq 0.05$; PAPC, $P < 0.001$. High fat atherogenic diet (Ath): lysoPC, $P < 0.0001$; PLPC, $P < 0.001$, PAPC, $P < 0.001$. Three or more preparations were analyzed per group.

The composition of CAST HDL was also distinctive as compared with common laboratory strains of mice, including B6. After isolation by sequential density gradient ultracentrifugation, the HDL from CAST mice were determined to have relatively low levels of phospholipids and cholesteryl esters but high levels of free cholesterol (Fig. 2, Table 1).

CAST mice have normal LCAT mRNA expression but reduced LCAT activity

The unusual composition and low levels of HDL cholesterol in CAST mice suggested that they may exhibit a deficiency of LCAT. Therefore, we examined LCAT activities in plasmas of CAST and B6 mice maintained on both chow and atherogenic diets. CAST mice exhibited decreased

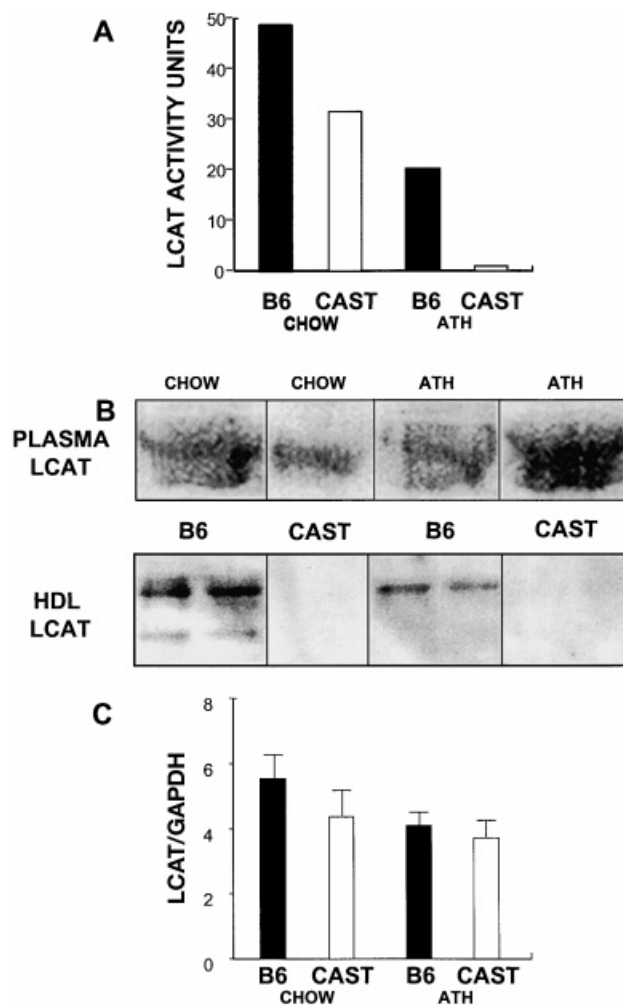


Fig. 3. CAST mice exhibit reduced plasma LCAT activity (A) and mass (B) but not mRNA (C). Female mice maintained on chow or high fat, atherogenic (Ath) diets ($n = 5$) were examined for plasma LCAT activity, plasma LCAT mass, and hepatic LCAT mRNA. LCAT activity (A) was assayed as described in Materials and Methods. LCAT mass in plasma (B) was determined by immunoblotting. Levels were not significantly different on chow ($P = 0.42$) or atherogenic ($P = 0.65$) diets. LCAT mass in ultracentrifugally isolated HDL (B) was determined by immunoblotting. In several such experiments no significant mass was observed in CAST mice. LCAT mRNA levels (C) (normalized to GAPDH mRNA levels) were estimated by Northern analysis.

TABLE 2. Sequence comparison of LCAT cDNA from CAST and B6 mice^a

| Nucleotide and Amino Acid Number | Mouse (B6) | Mouse (CAST) | Rat | Human |
|----------------------------------|------------|--------------|------------|------------|
| Nucleotide 63 | CTG | GTG | CTG | CTG |
| Amino acid 19 | L | V | L | L |
| Nucleotide 1242 | ATG | CTG | CTG | CTG |
| Amino acid 412 | M | L | L | L |

^a Liver mRNA for LCAT was reverse transcribed and amplified from CAST and B6 mice and sequenced in both directions. Differences in the sequence are indicated in bold face and the corresponding amino acids are shown.

levels, particularly on the atherogenic diet (Fig. 3A). To test whether the decreased activity was due to a reduced mass or a structural mutation of LCAT affecting activity, LCAT mass was quantitated with a monospecific antibody. The amount of LCAT detected in plasma by Western analysis was similar in CAST and B6 mice on both diets (Fig. 3B). Moreover, both strains exhibited similar levels of hepatic LCAT mRNA on both diets, indicating that a promoter variation of the LCAT gene is not involved (Fig. 3C).

One potential mechanism for the reduced LCAT activity is that the LCAT binds poorly to HDL, resulting in increased enzyme turnover and HDL depleted in cholesteryl esters. To examine this possibility we examined LCAT protein in HDL isolated by ultracentrifugation. In B6 mice, most of the plasma LCAT was associated with the ultracentrifugally isolated HDL, whereas in CAST mice, significantly lower levels were observed (Fig. 3B). Because the isolation of HDL by ultracentrifugation subjects the particles to high salt and pressure, we also examined the association of LCAT with HDL after FPLC analysis in 0.15 M NaCl. Under those low salt conditions, the levels of LCAT activity and mass associated with HDL were similar in

CAST and B6 mice (data not shown). Thus, CAST LCAT appears to be associated with HDL under physiologic conditions, but is dissociated in part under the conditions of ultracentrifugation.

To examine the possibility that structural differences in LCAT between the two strains contributed to a loss in high salt, hepatic LCAT cDNA was sequenced to check for possible mutations that could influence the function of the protein (Table 2). For this, hepatic mRNA was reverse transcribed and subjected to PCR amplification of specific regions of the LCAT-coding sequence. Two nucleotide changes were identified, but both of these resulted in relatively conservative amino acid changes, L19→V and M412→L. These data suggest that the deficiency in LCAT activity is most likely due to altered interaction of LCAT with HDL or other lipoproteins (see Discussion) in CAST mice. It is possible that this results from the above-described missense variations, although this seems unlikely given the conservative nature of the substitutions and the genetic data discussed below. Alternatively, CAST HDL or plasma may contain a factor or factors influencing the interaction of LCAT with HDL.

CAST mice exhibit adrenal lipid depletion

Because of the unusually low levels of HDL and cholesteryl esters in CAST mice, we examined whether the mice exhibited “adrenal lipid depletion” resulting from the failure of the adrenals to take up sufficient cholesterol from HDL (27). When CAST adrenals were sectioned and stained for cholesteryl esters with oil red O, a striking deficiency was observed as compared with B6 (Fig. 4). When fed an atherogenic diet, the content of cholesteryl esters in CAST adrenals increased substantially, although it remained considerably less than that of B6 mice. The increase in cholesterol levels occurred de-

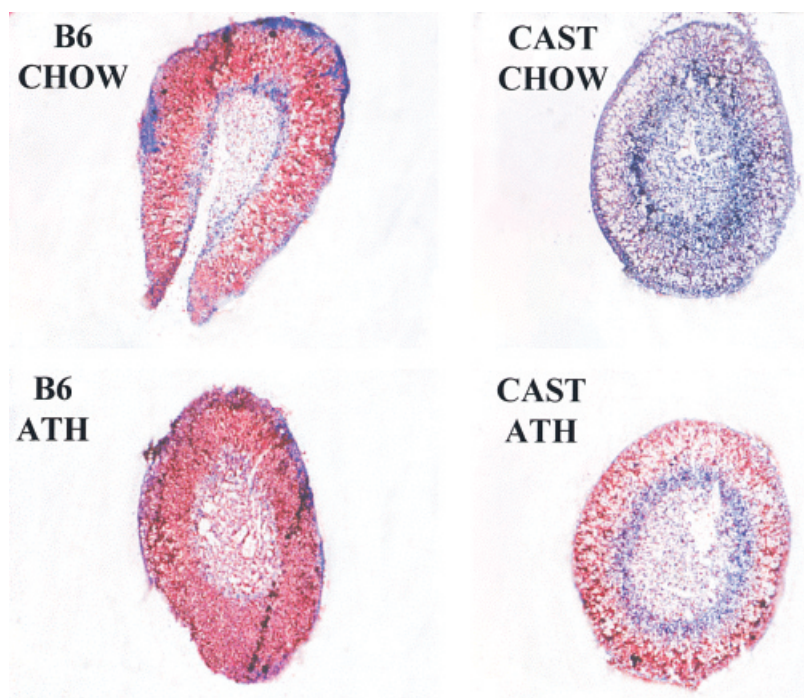


Fig. 4. CAST mice exhibit a form of adrenal lipid depletion. Adrenal glands from female mice 5 months of age, maintained on either chow or atherogenic diets, were cryosectioned and stained for cholesteryl esters using oil red O. The cortex normally stains intensely because of the presence of cholesteryl esters that serve as a pool of cholesterol for steroid hormone synthesis.

spite the fact that LCAT activity and HDL cholesterol decreased on the atherogenic diet. This may have resulted from the large increase in LDL/VLDL, which can also donate cholesterol to adrenals.

CAST VLDL exhibit panhandle-like protrusions

VLDL was isolated by ultracentrifugation from plasma of CAST and B6 mice on either chow or ATH diets. The average diameter of all the particles in both the CAST and B6 mice was between 119 and 123 nm. In the samples from the CAST mice on the ATH diet, more than 50% of the lipoprotein particles contained a single tail-like projection that extended on average about 45 nm from the surface of the particle (Fig. 5A). VLDL samples from the B6 mice on the ATH diet (Fig. 5B) or chow diet (not shown) were free of any lipid projections. VLDL from the CAST mice fed a chow diet were largely free of projections (only 1 particle with a projection was observed out of 50 grid square fields examined). Similar panhandle-like projections have been observed in LCAT-deficient mice (27), supporting the conclusion that CAST mice have a functional LCAT deficiency.

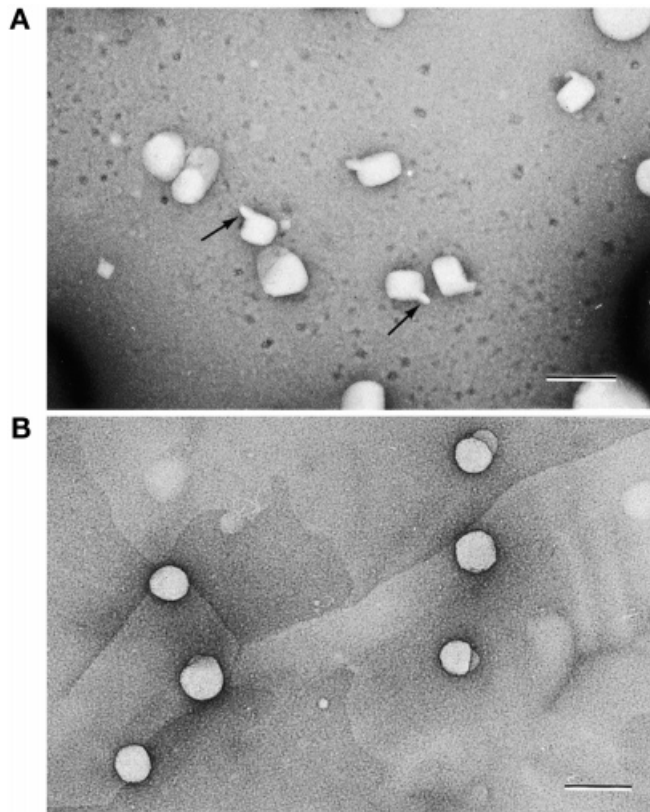


Fig. 5. Triglyceride-rich lipoproteins of CAST mice exhibit tail-like protrusions. Very low density lipoprotein (VLDL) fractions were isolated by density centrifugation. VLDL samples from CAST (A, original magnification $\times 41,698$) and B6 (B, original magnification $\times 40,614$) mice maintained on an atherogenic diet were subjected to negatively stained electron microscopy. The CAST particles were characterized by the common presence of panhandle-like protrusions (arrows). These results are representative of two separate VLDL preparations taken from mice, of each strain, on chow and on high fat diets.

TABLE 3. Sequence comparison of ApoA1 cDNA from CAST and B6 mice^a

| Nucleotide and Amino Acid Number | Mouse (B6) | Mouse (CAST) | Rat | Human |
|----------------------------------|------------|--------------|------------|------------|
| Nucleotide 361 | GTG | TTG | CTG | CTG |
| Amino acid 106 | V | L | L | L |
| Nucleotide 444 | AAA | AAT | AAC | CAG |
| Amino acid 133 | K | N | N | Q |
| Nucleotide 797 | GCC | CTC | ATC | TTC |
| Amino acid 253 | A | V | I | F |

^a Liver mRNA for apoA-I from B6 and CAST mice was reverse transcribed, amplified, and sequenced. Differences in the nucleotide sequence (in bold face) and predicted amino acid sequence are indicated.

ApoA-I levels are similar in CAST and B6 mice

Plasma and FPLC fractions containing HDL were examined for apoA-I levels by immunoblotting, using antibody to mouse apoA-I. There were no significant differences in apoA-I levels between CAST and B6 mice on either a chow or high fat diet (Table 1). Thus, although CAST mice have lower HDL cholesterol levels than B6 mice, they have similar levels of apoA-I in plasma and isolated HDL. Considering the reduced levels of cholesteryl esters and phospholipids in CAST HDL, these particles are apoA-I rich as compared with B6 HDL particles. There were no significant differences in either apoE or apoA-II between the four groups tested (data not shown). To determine whether apoA-I in CAST mice is structurally altered in a way that may result in poor LCAT binding and activation, we sequenced apoA-I in B6 and CAST mice (Table 3). For this, liver mRNA was reverse transcribed and specifically amplified by PCR. Three nucleotide changes were identified, all resulting in conservative amino acid changes (V106→L, K133→N, and A253→V).

Inheritance of HDL levels in CAST \times B6 intercross

F₁ mice from a cross of B6 and CAST mice exhibited plasma lipid parameters intermediate between the parental strains. For example, on a chow diet the levels of HDL cholesterol in female CAST, F₁, and B6 mice were 39 ± 4 , 42 ± 4 , and 46 ± 3 mg/dl, respectively, while the levels in male mice were 26 ± 4 , 47 ± 1 , and 53 ± 3 mg/dl. Figure 8 (below) shows the distributions of lipoprotein levels in about 290 (CAST \times B6)F₂ mice. Mice were examined on a low fat chow diet and also after challenge for 7 weeks with a high fat, atherogenic diet. The wide range of values, much larger than the variation observed in the parental and F₁ mice, indicates strong genetic influences. With the exception of triglyceride levels, the traits exhibited continuous, roughly normal distributions, consistent with polygenic inheritance (Fig. 6).

Genetic loci controlling HDL levels and related traits

A complete linkage map of all chromosomes except the Y chromosome was constructed with microsatellite markers at an average spacing of about 10 cM (21). Quantitative trait locus (QTL) analysis was performed with MAPMAKER/QTL software. Statistical criteria used for determining the significance of QTL results were those proposed by Lander

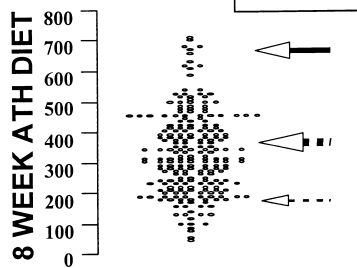
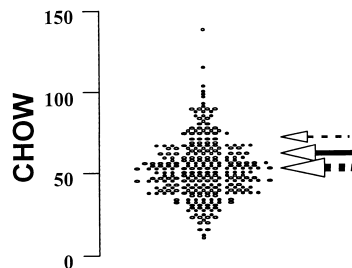
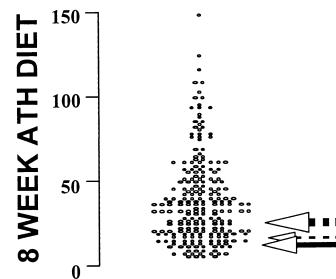
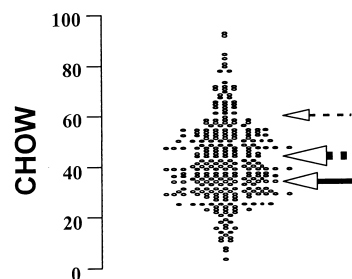
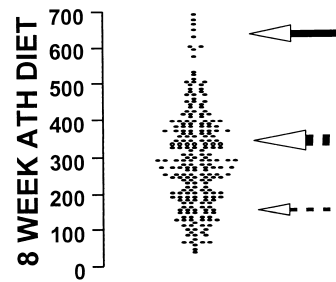
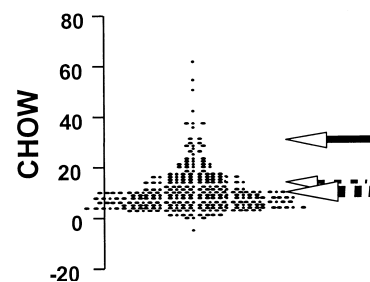
TOTAL CHOLESTEROL**HDL CHOLESTEROL****LDL/VLDL CHOLESTEROL**

Fig. 6. Frequency distributions of plasma lipoprotein levels in $(B6 \times CAST)F_2$ mice. Each point represents an individual mouse. The filled arrows represent average values for the CAST parent; thin hatched arrows, average values for B6 mice; thick hatched arrows, average values for $(B6 \times CAST)F_1$ mice.

and Kruglyak (28). For an F_2 intercross, suggestive linkage is indicated by LOD scores >2.8 and significant linkage is indicated by LOD scores >4.3 . A total of 12 loci for HDL cholesterol with LOD scores exceeding 3.3 were identified for the two diets (Table 4). Many of the loci yielded much higher LOD scores with one diet than the other, suggesting genetic-dietary interactions.

The two QTLs on chromosome 2 affect HDL cholesterol on chow as well as the high fat diet (Table 4). These loci colocalize with loci for body fat and insulin levels, as previously reported (21). One candidate gene within the proximal chromosome 2 QTL is the PLTP gene. To test whether this gene could explain the QTL, PLTP activity was determined in plasmas of F_2 animals. The activity did not, however, segregate with the chromosome 2 locus (data not shown), indicating that the PLTP gene is unlikely to underlie the locus. Because lipoprotein levels have clearly been associated with body fat in genetic-epidemiologic studies, it seems likely that the chromo-

some 2 loci result from metabolic interactions involving adipose tissue.

A QTL for HDL cholesterol was observed on chromosome 5 (LOD score 6.1) in a region in which QTLs for HDL have previously been observed in crosses between strains B6 and C3H/HeJ and between SM/J and NZB/BINJ (Fig. 7). A candidate gene, encoding the HDL receptor SR-BI, resides at the distal locus. To investigate the possible involvement of the locus, SR-BI expression was examined in the parental strains at the level of mRNA and the level of protein (see Fig. 10). B6 mice had significantly higher levels of SR-BI mRNA in liver than CAST mice on both chow and high fat diets (Table 1). Nevertheless, no significant differences were observed at the level of protein in multiple experiments (Table 1). To test whether CAST and B6 mice differ in SR-BI protein sequence such that function may be altered, we sequenced the cDNA. Reverse transcriptase-PCR amplification of hepatic mRNA was used to prepare sequencing templates. The results revealed three nucle-

TABLE 4. Effects of genotype on linked parameters^a

| Locus | Diet | Parameter | BB | CB | CC | LOD |
|------------------|------|-------------------|--------------|--------------|--------------|-----|
| Chromosome 2 | | | | | | |
| <i>D2MIT9</i> | Chow | HDL cholesterol | 45.0 ± 2.0 | 43.0 ± 2.0 | 38.0 ± 2.0 | 0.6 |
| | Ath | HDL cholesterol | 52.4 ± 4.1 | 35.5 ± 2.1 | 29.8 ± 2.6 | 5.6 |
| Chromosome 2 | | | | | | |
| <i>D2MIT50</i> | Chow | HDL cholesterol | 45.0 ± 2.0 | 44.0 ± 1.0 | 36.0 ± 2.0 | 3.5 |
| | Ath | HDL cholesterol | 49.0 ± 6.0 | 42.0 ± 3.0 | 28.3 ± 3.0 | 3.4 |
| Chromosome 3 | | | | | | |
| <i>D2MIT12</i> | Chow | Total cholesterol | 61.2 ± 2.7 | 51.9 ± 1.6 | 49.1 ± 1.5 | 3.5 |
| | | HDL cholesterol | 49.4 ± 2.2 | 41.1 ± 1.4 | 38.1 ± 1.3 | 4.2 |
| Chromosome 5 | | | | | | |
| <i>D5MIT10</i> | Ath | HDL cholesterol | 25.3 ± 2.3 | 39.8 ± 2.4 | 46.9 ± 3.7 | 6.0 |
| <i>D5MIT27</i> | Ath | HDL cholesterol | 30.6 ± 3.0 | 38.3 ± 2.3 | 46.5 ± 4.1 | 3.8 |
| Chromosome 8 | | | | | | |
| <i>D8MIT12</i> | Chow | HDL cholesterol | 48.5 ± 2.0 | 39.8 ± 1.2 | 38.8 ± 2.1 | 3.6 |
| <i>D8MIT14</i> | Chow | HDL cholesterol | 47.5 ± 2.0 | 41.1 ± 1.2 | 37.9 ± 1.8 | 3.5 |
| Chromosome 9 | | | | | | |
| <i>D9MIT2</i> | Chow | Total cholesterol | 47.7 ± 2.2 | 53.2 ± 1.5 | 57.8 ± 2.1 | 3.3 |
| | Chow | HDL cholesterol | 36.9 ± 2.0 | 42.3 ± 1.3 | 46.0 ± 1.7 | 4.2 |
| Chromosome 14 | | | | | | |
| <i>D14MIT2</i> | Chow | HDL cholesterol | 43.5 ± 1.7 | 42.8 ± 1.2 | 34.7 ± 2.4 | 3.4 |
| Chromosome 16 | | | | | | |
| <i>D16MIT3</i> | Chow | HDL cholesterol | 45.7 ± 1.6 | 43.6 ± 1.4 | 35.0 ± 1.6 | 4.4 |
| Chromosome 17 | | | | | | |
| <i>D17MIT7</i> | Ath | HDL cholesterol | 30.2 ± 2.7 | 35.8 ± 2.0 | 55.2 ± 4.8 | 6.5 |
| Chromosome 18 | | | | | | |
| <i>D18MIT142</i> | Ath | HDL cholesterol | 48.7 ± 3.8 | 33.6 ± 2.1 | 35.4 ± 3.2 | 3.8 |
| Chromosome 19 | | | | | | |
| <i>D19MIT5</i> | Ath | Total cholesterol | 310.1 ± 14.2 | 321.2 ± 12.8 | 394.5 ± 24.3 | 3.3 |

Significant QTLs observed in the (B6 × CAST)_{F2} genetic cross are summarized. The levels of HDL cholesterol or total cholesterol (mg/dl) for F₂ mice of genotype BB (homozygous B6), CB (heterozygous), and CC (homozygous CAST) are indicated along with the maximum likelihood of observed data score.

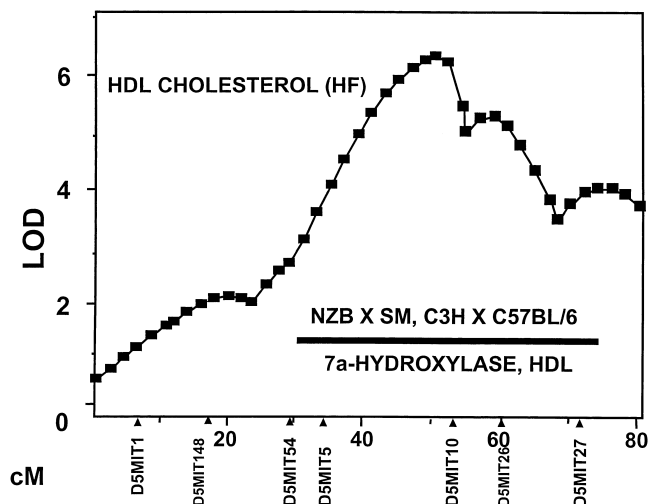


Fig. 7. QTLs on chromosome 5 for HDL cholesterol levels in mice on an atherogenic diet. Shown is a plot generated by the MAPMAKER/QTL program for likelihood of observed data (LOD) scores along chromosome 5 in the (B6 × CAST)_{F2} cross. Shown at the bottom are markers typed in the F₂ cross. The bar indicates the location of QTLs for HDL cholesterol previously identified in genetic crosses between strains NZB and SM (16) and strains C3H and C57BL/6 (20) and for 7 α -hydroxylase expression in a genetic cross between strains C3H and C57BL/6.

otide substitutions, none of which altered the amino acid sequence (Table 5). The results indicate that the QTL is not due to SR-BI gene variation despite its prominent role in HDL metabolism.

The QTL on chromosome 8 is located over the gene for LCAT. As shown in Fig. 3, LCAT activity was reduced in CAST mice as compared with B6 mice, supporting its potential involvement. Interestingly, the locus also appeared to segregate with the levels of plasma PLTP (Fig. 8). Because the PLTP gene is located on mouse chromosome 2, the finding cannot be due to variations of the PLTP structural gene. As discussed above, the deficiency of LCAT results from a posttranslational mechanism, because CAST mice have normal levels of LCAT mRNA. Thus, the reduced levels of LCAT presumably result from factors interacting with LCAT that are required for its stability or interaction with HDL.

A QTL on chromosome 16 for HDL cholesterol is located over the gene for apoD (Fig. 9). Immunoblotting plasma samples using antibody against human apoD did not reveal significant differences between the two strains of mice on either a chow or high fat diet (data not shown).

A strong QTL for HDL levels (LOD score 6.4) was observed on chromosome 17 (Fig. 10). We had mapped the

TABLE 5. Sequence comparison of SR-BI cDNA from B6 and CAST mice^a

| Nucleotide and Amino Acid Number | Mouse (B6) | Mouse (CAST) | Rat | Human |
|----------------------------------|------------|--------------|-----|-------|
| Nucleotide 354 | CCG | CCC | CCC | CCC |
| Amino acid 48 | P | P | P | P |
| Nucleotide 390 | CCC | CCA | CCT | CCT |
| Amino acid 60 | P | P | P | P |
| Nucleotide 1271 | TTG | CTG | CTG | CTG |
| Amino acid 354 | L | L | L | L |

^a Liver mRNA for SR-BI was reverse transcribed, amplified, and sequenced in both directions. All sequence differences, (in bold face) and predicted amino acids are indicated.

gene for PAF-AH to this region of chromosome 17 by linkage analysis (A. J. Lusis, unpublished observations). However, PAF-AH levels were similar among parental strains (Table 1), indicating that it is unlikely to be involved. A second possible QTL was observed near the terminus of chromosome 17, but it did not contain an obvious candidate gene.

DISCUSSION

We have examined genetic factors contributing to variations in HDL levels and compositions in studies of two highly divergent strains of mice, CAST and B6. On a chow diet, CAST mice exhibited reduced levels of HDL as compared with other common strains examined. The composition of the HDL was also unusual, as it had a surface unusually rich in free cholesterol and poor in phospholipids. Our results indicated that these differences were due in part to a functional deficiency of plasma LCAT. On an atherogenic diet, CAST mice had low levels of HDL and

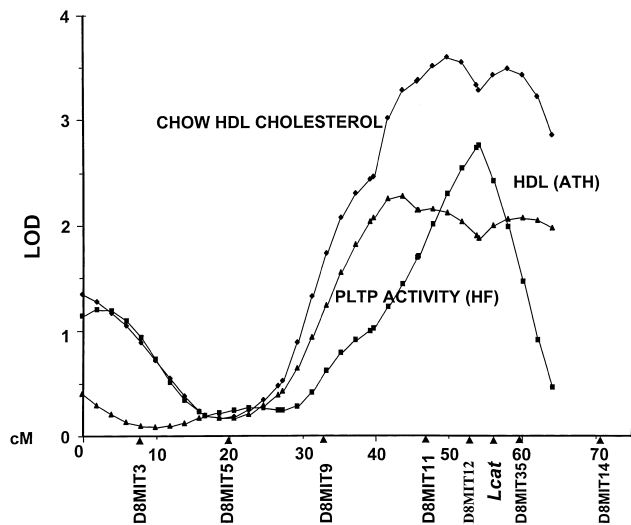


Fig. 8. QTLs on chromosome 8 for plasma HDL cholesterol [chow and high fat (HF) diets] and PLTP activity (HF). These LOD score plots along chromosome 8 were generated for F₂ mice using the MAPMAKER/QTL program. The locations of typed genetic markers and the LCAT candidate gene are indicated at the bottom.

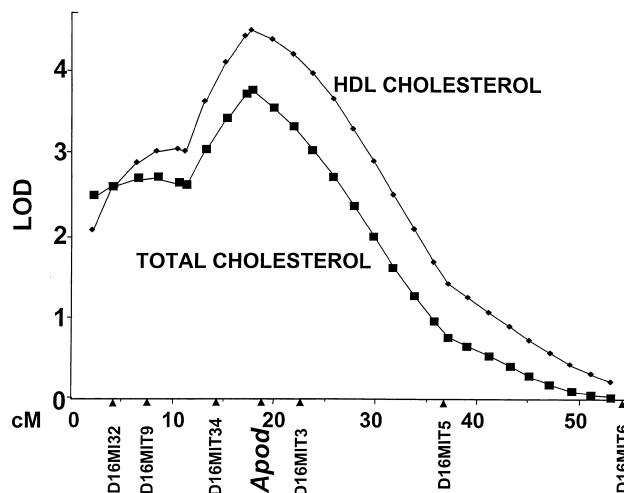


Fig. 9. QTLs on chromosome 16 for plasma HDL cholesterol and total cholesterol on a chow diet. The location of genetic markers and the apoD gene are indicated on the bottom.

high levels of LDL/VLDL. Analysis of an F₂ intercross between CAST and B6 mice yielded two significant conclusions relating to the genetic control of HDL. First, numerous genes contributed to variations in HDL levels. Second, most of the observed variation was not explained by the usual candidate genes, such as apolipoproteins, lipoprotein receptors, or enzymes involved in HDL metabolism.

Our studies have revealed an interesting mechanism contributing to the low levels of HDL cholesterol in CAST mice. Although the mice express about the same levels of LCAT mRNA as B6 and other strains (29), there is reduced enzyme activity in the plasma. This deficiency appears to result in part from an altered interaction of LCAT with HDL particles. The nature of this reduced interaction is unclear, although it seems likely to result from the composition of the HDL rather than an alteration of the

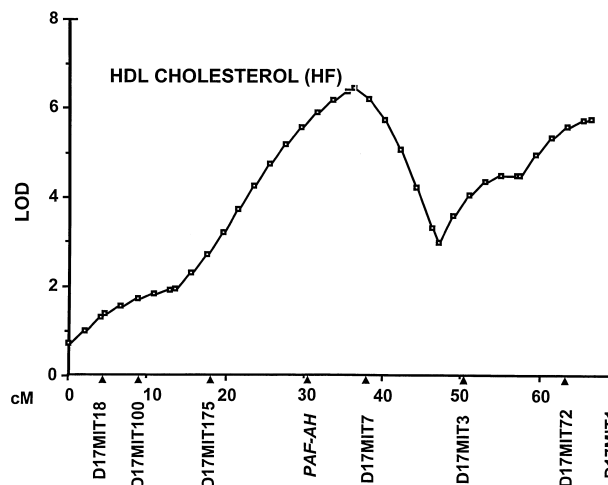


Fig. 10. Chromosome 17 QTL for HDL cholesterol levels. Shown are the LOD score plots for HDL cholesterol on an atherogenic diet. The locations of genetic markers and the PAF-AH gene are indicated along the bottom.

LCAT protein. Sequencing of the LCAT mRNA revealed only two, conservative, amino acid substitutions in CAST versus B6 mice (Table 2), and only a small fraction of the variance of HDL cholesterol levels could be attributed to the LCAT locus on chromosome 8 (Table 4). Another possibility is that a significant proportion of cholesteryl esters in mouse plasma are generated on apoB-containing lipoproteins and that this process is defective in CAST mice. CAST mice exhibit unusually high levels of LDL/VLDL cholesterol and, in CAST mice, the plasma ratio of unesterified cholesterol to total cholesterol (UC/TC ratio) is elevated more than the HDL UC/TC ratio (Table 1). This could result from altered interaction of LCAT with apoB-containing lipoproteins in CAST mice.

The functional deficiency of LCAT in CAST mice was supported by two related phenomena observed in LCAT-deficient mice: adrenal lipid depletion and VLDL panhandle protrusions. Adrenal lipid depletion is characterized by severely depleted stores of cholesteryl esters in the adrenal gland. In the case of CAST mice, it is likely that the depletion results from the low levels of HDL cholesterol in the circulation, because the bulk of the adrenal cholesterol esters are derived by uptake from HDL (27). Another form of adrenal lipid depletion, occurring in strain AKR mice, results from the failure to esterify cholesterol due to a deficiency of acyl-CoA:cholesterol acyltransferase (30). VLDL "panhandles" similar to those observed in CAST mice are also observed in LCAT-deficient mice, suggesting that LCAT deficiency is the cause of the panhandles (27). Human LCAT deficiency results in renal problems, but inspection of kidney sections of CAST mice did not reveal evidence of pathology.

In this study, we also performed QTL analysis in an effort to identify genetic factors influencing HDL levels. Our studies revealed about a dozen QTLs influencing HDL levels, most not corresponding to any obvious candidate genes. Some of these loci had been observed in previous genetic crosses, including the chromosome 2 and chromosome 5 loci (16, 20), but most were novel. Altogether, more than 20 loci for HDL levels with significant LOD scores have been observed in various mouse crosses (16, 20, 21, 31) and this study. The identification of the Tangier disease gene revealed a novel pathway for regulation of HDL metabolism (8–10). Also, mutations of the leptin gene have been found to alter the localization of HDL to the endosomal recycling compartment in isolated hepatocytes (32). Our results suggest that there are additional, as yet unknown, genes that contribute importantly to HDL metabolism.

In addition to providing a view of the overall complexity of HDL metabolism, our results provide an approach for the identification of new genetic factors affecting HDL metabolism in mice and humans. If the QTLs contain candidate genes, these can be tested for possible involvement. In this study, we examined several candidates, including SR-BI, apoA-I, LCAT, PLTP, and PAF-AH. All exhibited similar levels of expression between CAST and B6 mice, and the cDNA sequences of SR-BI, apoA-I, and LCAT exhibited either no amino acid substitutions or conservative

substitutions. Thus, these candidates are unlikely to explain the QTLs. In the absence of candidate genes, it is possible, in the mouse, to isolate individual chromosomal regions harboring QTLs from one strain onto the background of a second strain, in congenic strains. Thus, a congenic strain would differ from the background strain at only a single locus contributing to the trait of interest. Such congenic strains can be utilized to examine interactions between the loci and, in principle, to perform fine structure mapping and eventual positional cloning of the gene underlying the QTL. We are presently in the process of constructing congenic strains for the various QTLs identified in this article. Finally, the QTLs can be utilized to direct genetic searches of loci contributing to human HDL metabolism. For example, the distal chromosome 2 locus reported here was originally observed in a genetic cross between strains NZB/BINJ and SM/J. On this basis, the locus was used to predict that human chromosome 20q may harbor a locus contributing to body fat and insulin levels. Indeed, when genetic markers on human chromosome 20q were used for linkage analysis in 152 pedigrees typed for measures of obesity, significant linkage was observed with insulin levels and body fat (33).

In the case of CAST mice, a particularly interesting variation for future studies involves the interaction of LCAT with lipoproteins. As discussed above, our biochemical and genetic results suggest that the chromosome 8 QTL containing the LCAT gene is not involved, although this requires further testing. Which, if any, of the other QTLs observed in this study is responsible is unclear, because at the time the genetic cross was set up, the HDL-LCAT interaction trait was unknown. To answer this question, additional QTL studies with CAST and B6 mice will have to be performed, with each backcross or F₂ progeny assessed for the trait. Of course, it is possible that multiple loci control the interaction of LCAT with HDL.

In conclusion, it appears that our understanding of common variations influencing HDL levels and composition is incomplete, because highly significant QTLs for HDL levels were observed in several chromosomal regions not containing any obvious candidate genes. Our results suggest one novel genetic variation possibly affecting the interaction of LCAT with HDL. This variation requires further biochemical and genetic characterization, but it is interesting to speculate that similar variations may occur in human populations. ■

These studies were supported in part by NIH grant HL30568 (A.J.L., A.M.F.), HL28481 (L.W.C.), and HL30086 (J.J.A.), and by the Laubisch Fund, UCLA. We thank J. Berliner, C. Fielding, and B. Brewer for advice and Rosa Chen for help in the preparation of this manuscript.

Manuscript received 20 April 2000 and in revised form 15 August 2000.

REFERENCES

1. Rhoads, G. G., C. L. Gulbrandsen, and A. Kugan. 1976. Serum lipoproteins and coronary artery disease in a population study of Hawaii Japanese men. *N. Engl. J. Med.* **294**: 293–298.

2. Castellani, L. W., M. Navab, B. J. Van Lenten, C. C. Hedrick, S. Y. Hama, A. M. Goto, A. M. Fogelman, and A. J. Lusis. 1997. Overexpression of apolipoprotein AII in transgenic mice converts high density lipoproteins to proinflammatory particles. *J. Clin. Invest.* **100**: 464–474.
3. Havel, R. J., J. P. Kane, and M. L. Kashyae. 1973. Interchange of apolipoproteins between chylomicrons and high density lipoproteins during alimentary lipemia in man. *J. Clin. Invest.* **52**: 32–38.
4. Tall, A. R., P. H. R. Green, R. M. Glickman, and J. W. Riley. 1979. Metabolic fate of chylomicron phospholipids and apoproteins in the rat. *J. Clin. Invest.* **64**: 977–989.
5. Hamilton, R. H., M. C. Williams, C. J. Fielding, and R. J. Havel. 1976. Discoidal bilayer structure of nascent high density lipoproteins from perfused rat liver. *J. Clin. Invest.* **58**: 667–680.
6. Brinton, E. A., S. Eisenberg, and J. L. Breslow. 1994. Human HDL cholesterol levels are determined by apoA-I fractional catabolic rate, which correlates inversely with estimates of HDL particle size. Effects of gender, hepatic and lipoprotein lipases, triglyceride and insulin levels, and body fat distribution. *Arterioscler. Thromb.* **14**: 707–720.
7. Cohen, J. C., G. L. Vega, and S. M. Grundy. 1999. Hepatic lipase: new insights from genetic and metabolic studies. *Curr. Opin. Lipidol.* **10**: 259–267.
8. Bodzioch, M., E. Orso, J. Klucken, T. Langmann, A. Böttcher, W. Diederich, W. Drobnik, S. Barlage, C. Büchler, M. Porsch-Özcürümez, W. E. Kaminski, H. W. Hahmann, K. Oette, G. Rothe, C. Aslanidis, K. J. Lackner, and G. Schmitz. 1999. The gene encoding ATP-binding cassette transporter 1 is mutated in Tangier disease. *Nat. Genet.* **22**: 347–351.
9. Brooks-Wilson, A., M. Marcil, S. M. Clee, L-H. Zhang, K. Roomp, M. van Dam, L. Yu, C. Brewer, J. A. Collins, O. F. Molhuizen, O. Loubser, B. F. F. Ouelette, K. Fichter, K. J. D. Ashbourne-Excoffon, C. W. Sensen, S. Scherer, S. Mott, M. Denis, D. Martindale, J. Frohlich, K. Morgan, B. Koop, S. Pimstone, J. J. P. Kastelein, J. Genest, Jr., and M. R. Hayden. 1999. Mutations in ABC1 in Tangier disease and familial high-density lipoprotein deficiency. *Nat. Genet.* **22**: 336–345.
10. Rust, S., M. Rosier, H. Funke, J. Real, Z. Amoura, J. C. Piette, J. F. Deleuze, H. B. Brewer, N. Duverger, P. Deneffe, and G. Assmann. 1999. Tangier disease is caused by mutations in the gene encoding ATP-binding cassette transporter 1. *Nat. Genet.* **22**: 352–355.
11. Lander, E. S., and N. J. Schork. 1994. Genetic dissection of complex traits. *Science*. **265**: 2037–2048.
12. Lusis, A. J., B. A. Taylor, R. W. Wangenstein, and R. C. LeBoeuf. 1983. Genetic control of lipid transport in mice. II. Genes controlling structure of high density lipoproteins. *J. Biol. Chem.* **258**: 5071–5078.
13. Paigen, B., D. Mitchell, K. Reue, A. Morrow, A. J. Lusis, and R. C. LeBoeuf. 1987. *Ath-1*, a gene determining atherosclerosis susceptibility and high density lipoprotein levels in mice. *Proc. Natl. Acad. Sci. USA*. **84**: 3763–3767.
14. Doolittle, M. H., R. C. LeBoeuf, C. H. Warden, L. M. Bee, and A. J. Lusis. 1990. A polymorphism affecting apolipoprotein A-II translational efficiency determines high density lipoprotein size and composition. *J. Biol. Chem.* **265**: 16380–16388.
15. Mehrabian, M., J-H. Qiao, R. H. Hyman, D. Ruddle, C. Laughton, and A. J. Lusis. 1993. Influence of the apoA-II gene locus on HDL levels and fatty streak development in mice. *Arterioscler. Thromb.* **13**: 1–10.
16. Purcell-Huynh, D. A., A. Weinreb, L. W. Castellani, M. Mehrabian, M. H. Doolittle, and A. J. Lusis. 1995. Genetic factors in lipoprotein metabolism: analysis of a genetic cross between inbred mouse strains NZB/BINJ and SM/J using a complete linkage map approach. *J. Clin. Invest.* **96**: 1845–1858.
17. Warden, C. H., J. S. Fislser, S. M. Shoemaker, P-Z. Wen, K. L. Svenson, M. J. Pace, and A. J. Lusis. 1995. Identification of four chromosomal loci determining obesity in a multifactorial mouse model. *J. Clin. Invest.* **95**: 1545–1552.
18. Shih, D. M., L. Gu, S. Hama, Y. Xia, M. Navab, A. M. Fogelman, and A. J. Lusis. 1996. Genetic-dietary regulation of serum paraoxonase expression and its role in atherogenesis in a mouse model. *J. Clin. Invest.* **97**: 1630–1639.
19. Welch, C. L., Y-R. Xia, I. Shechter, R. Farese, M. Mehrabian, S. Mehdizadeh, C. H. Warden, and A. J. Lusis. 1996. Genetic regulation of cholesterol homeostasis: chromosomal organization of candidate genes. *J. Lipid Res.* **37**: 1406–1421.
20. Machleder, D., B. Ivandic, C. L. Welch, L. Castellani, K. Reue, and A. J. Lusis. 1997. Complex genetic control of HDL levels in mice in response to an atherogenic diet: coordinate regulation of HDL levels and bile acid metabolism. *J. Clin. Invest.* **99**: 1406–1419.
21. Mehrabian, M., P-Z. Wen, J. Fislser, R. C. Davis, and A. J. Lusis. 1998. Genetic loci controlling body fat, lipoprotein metabolism, and insulin levels in a multifactorial mouse model. *J. Clin. Invest.* **101**: 2485–2496.
22. Miyazaki, A., A. T. Rahim, T. Ohta, Y. Morino, and S. Horiuchi. 1992. High density lipoprotein mediates selective reduction in cholesteryl esters from macrophage foam cells. *Biochim. Biophys. Acta.* **1126**: 73–80.
23. Cheung, M. C., G. Wolfbauer, and J. J. Albers. 1996. Plasma phospholipid mass transfer rate: relationship to plasma phospholipid and cholesteryl ester transfer activities and lipid parameters. *Biochim. Biophys. Acta.* **1303**: 103–110.
24. Hedrick, C. C., L. W. Castellani, C. H. Warden, D. L. Puppione, and A. J. Lusis. 1993. Influence of mouse apolipoprotein A-II on plasma lipoproteins in transgenic mice. *J. Biol. Chem.* **268**: 676–682.
25. Manly, K. F. 1993. A Macintosh program for storage and analysis of experimental genetic mapping data. *Mamm. Genome*. **4**: 303–313.
26. Lander, E. S., P. Green, J. Abrahamson, A. Barlow, M. Daley, S. Lincoln, and L. Newburg. 1987. MAPMAKER: an interactive computer package for constructing primary genetic linkage maps of experimental and natural populations. *Genomics*. **1**: 174–181.
27. Ng, D. S., O. L. Francone, T. M. Forte, J-L. Zhang, M. Haghpassand, and E. M. Rubin. 1997. Disruption of murine lecithin:cholesterol acyltransferase gene causes impairment of adrenal lipid delivery and up-regulation of scavenger receptor class B type I. *J. Biol. Chem.* **272**: 15777–15781.
28. Lander, E. S., and L. Kruglyak. 1995. Genetic dissection of complex traits: guidelines for interpreting and reporting linkage results. *Nat. Genet.* **11**: 241–247.
29. Warden, C. H., C. Langer, J. I. Gordon, B. A. Taylor, J. W. McLean, and A. J. Lusis. 1989. Tissue specific expression, developmental regulation and chromosomal mapping of the lecithin-cholesterol acyl transferase gene: evidence for expression in brain and testes as well as liver. *J. Biol. Chem.* **264**: 21573–21581.
30. Meiner, V. L., C. L. Welch, S. Cases, H. M. Meyers, E. Sande, A. J. Lusis, and R. V. Farese, Jr. 1998. Adrenocortical lipid depletion gene (*ald*) in AKR mice is associated with acyl-CoA:cholesterol acyltransferase (ACAT) mutation. *J. Biol. Chem.* **273**: 1064–1069.
31. Gu, L., M. W. Johnson, and A. J. Lusis. 1999. Quantitative trait locus analysis of plasma lipoprotein levels in an autoimmune mouse model: interactions between lipoprotein, autoimmune disease, and atherogenesis. *Arterioscler. Thromb. Vasc. Biol.* **19**: 442–453.
32. Silver, D. L., N. Wang, and A. R. Tall. 2000. Defective HDL particle uptake in *ob/ob* hepatocytes causes decreased recycling, degradation and selective lipid uptake. *J. Clin. Invest.* **105**: 151–159.
33. Lemberas, A. V., L. Perusse, Y. C. Chagnon, J. S. Fislser, C. H. Warden, D. A. Purcell-Huynh, F. T. Dionne, J. Gagnon, A. Nadeau, A. J. Lusis, and C. Bouchard. 1997. Identification of an obesity quantitative trait locus on mouse chromosome 2 and evidence of linkage to body fat and insulin on the human homologous region 20q. *J. Clin. Invest.* **100**: 1240–1247.